2015

Novel mode of ISG15-mediated protection against influenza A virus and Sendai virus in mice

David J. Morales
Washington University School of Medicine in St. Louis

Kristen Monte
Washington University School of Medicine in St. Louis

Lulu Sun
Washington University School of Medicine in St. Louis

Jessica J. Struckhoff
Washington University School of Medicine in St. Louis

Eugene Agapov
Washington University School of Medicine in St. Louis

See next page for additional authors

Authors
David J. Morales, Kristen Monte, Lulu Sun, Jessica J. Struckhoff, Eugene Agapov, Michael J. Holtzman, Thaddeus S. Stappenbeck, and Deborah J. Lenschow

JVI Journals.ASM.org

Novel Mode of ISG15-Mediated Protection against Influenza A Virus and Sendai Virus in Mice

David J. Morales,[a] Kristen Monte,[a] Lulu Sun,[c] Jessica J. Struckhoff,[a] Eugene Agapov,[a] Michael J. Holtzman,[a,b] Thaddeus S. Stappenbeck,[c] Deborah J. Lenschow[a,c]

Department of Internal Medicine,[a] Department of Cell Biology,[b] and Department of Pathology and Immunology,[c] Washington University School of Medicine, St. Louis, Missouri, USA

ABSTRACT

ISG15 is a diubiquitin-like modifier and one of the most rapidly induced genes upon type I interferon stimulation. Hundreds of host proteins and a number of viral proteins have been shown to be ISGylated, and understanding how these modifications affect the interferon response and virus replication has been of considerable interest. ISG15$^{-/-}$ mice exhibit increased susceptibility to viral infection, and in the case of influenza B virus and vaccinia virus, ISG15 conjugation has been shown to restrict virus replication *in vivo*. A number of studies have also found that ISG15 is capable of antagonizing replication of some viruses in tissue culture. However, recent findings have demonstrated that ISG15 can protect mice from Chikungunya virus infection without affecting the virus burden. In order to better understand the function of ISG15 *in vivo*, we characterized the pathogenesis of influenza A virus and Sendai virus in ISG15$^{-/-}$ mice. We found that ISG15 protects mice from virus induced lethality by a conjugation-dependent mechanism in both of these models. However, surprisingly, we found that ISG15 had minimal effect on virus replication and did not have an obvious role in the modulation of the acute immune response to infection. Instead, we observed an increase in the number of diseased small airways in mice lacking ISG15. This ability of ISG15 to protect mice in a conjugation-dependent, but nonantiviral, manner from respiratory virus infection represents a previously undescribed role for ISG15 and demonstrates the importance of further characterization of ISG15 *in vivo*.

IMPORTANCE

It has previously been demonstrated that ISG15$^{-/-}$ mice are more susceptible to a number of viral infections. Since ISG15 is one of the most strongly induced genes after type I interferon stimulation, analysis of ISG15 function has largely focused on its role as an antiviral molecule during acute infection. Although a number of studies have shown that ISG15 does have a small effect on virus replication in tissue culture, few studies have confirmed this mechanism of protection *in vivo*. In these studies we have found that while ISG15$^{-/-}$ mice are more susceptible to influenza A virus and Sendai virus infections, ISGylation does not appear to mediate this protection through the direct inhibition of virus replication or the modulation of the acute immune response. Thus, in addition to showing a novel mode of ISG15 mediated protection from virus infection, this study demonstrates the importance of studying the role of ISG15 *in vivo*.

During acute infection, the survival of an organism is dependent on both its ability to inhibit pathogen replication, thus reducing pathogen burden, and its ability to tolerate the ensuing tissue damage incurred both from the pathogen itself, as well as from the immune response mounted against the pathogen (1, 2). Limiting pathogen replication and eventual pathogen clearance is dependent on both the innate and the adaptive immune responses. Of the many genes induced after viral infection, type I interferons are among the most rapidly and robustly expressed genes and play a critical role in modulating the immune response to viral infections (3–5).

After detection of viruses through pathogen recognition receptors, type I interferons are released from cells and subsequently bind to their cell surface receptors (IFNAR1/IFNAR2) in both an autocrine and paracrine fashion. Signaling through the type I interferon receptors induces the expression of hundreds of genes classified as interferon-stimulated genes (ISGs). A subset of ISGs directly inhibit different steps of virus replication, and it is through the collective action of these ISGs that type I interferons convert cells into what has classically been described as an antiviral state (6). In addition, type I interferons play a role in the regulation of both innate and adaptive immune cell responses to infection (7). These include their ability to induce natural killer (NK) cell activation, enhance antigen presentation activity by dendritic cells and aid in the development and maintenance of CD8$^+$ T cell memory, and antibody responses. Therefore, type I interferons regulate a range of host responses that impact disease outcome.

Interferon-stimulated gene 15 (ISG15) is one of the most rapidly and robustly induced genes upon type I interferon stimulation (8, 9). ISG15 is an ubiquitin-like modifier containing two ubiquitin-like domains that share ca. 30% amino acid sequence homology to ubiquitin. ISG15 is expressed as a 17-kDa precursor

Received 18 July 2014 **Accepted** 7 October 2014

Accepted manuscript posted online 15 October 2014

Citation Morales DJ, Monte K, Sun L, Struckhoff JJ, Agapov E, Holtzman MJ, Stappenbeck TS, Lenschow DJ. 2015. Novel mode of ISG15-mediated protection against influenza A virus and Sendai virus in mice. J Virol 89:337–349. doi:10.1128/JVI.02110-14.

Editor: S. Perlman

Address correspondence to Deborah J. Lenschow, dlenscho@dom.wustl.edu.

doi:10.1128/JVI.02110-14

protein that is proteolytically processed at its C terminus to expose an LRLRGG amino acid motif through which it covalently conjugates to lysine residues of target proteins (10, 11). ISGylation of target proteins occurs through an enzymatic cascade similar to that of ubiquitin conjugation, involving an E1 activating enzyme, an E2 conjugating enzyme, and an E3 ligase (12–17). Proteomic studies have identified hundreds of proteins as being ISGylated after interferon stimulation or capable of being ISGylated in an overexpression system (18, 19). However, the effects of relatively few of these modifications have been studied, and it remains unclear what the functional consequence of ISGylation is for most ISGylated targets.

To date, the most striking phenotype that has been described in ISG15-deficient mice is their increased susceptibility to viral infections, ranging from influenza viruses to herpes simplex virus 1 (HSV-1), Chikungunya virus (CHIKV), vaccinia virus, and Sindbis virus (20–23). Consequently, ISG15 has been hypothesized to protect the host from virus-induced lethality by acting as an antiviral molecule and directly inhibiting viral replication. Indeed, initial studies into the mechanism by which ISG15 mediates protection supported a role for ISG15 in directly antagonizing the virus life cycle. We have shown that influenza B virus replicates to 100-fold-greater levels in the lungs of ISG15$^{-/-}$ deficient mice compared to WT mice (21). This inhibition of replication was dependent on the ability of ISG15 to form conjugates as increased influenza B virus replication was also seen in mice that lack the ISG15 E1 activating enzyme, UbE1L, and thus fail to form ISG15 conjugates (24). Subsequent studies have demonstrated that ISG15 can antagonize the replication of vaccinia virus, influenza A virus, Sendai virus, human papillomavirus, Ebola virus, and HIV-1 in tissue culture to various degrees (23, 25–33).

However, recent evidence has shown that the role of ISG15 during infection is not limited to conjugation-dependent inhibition of virus replication. The nonconjugated ("free") form of ISG15 protects mice against CHIKV by regulating cytokine production during infection. In this model, ISG15$^{-/-}$, but not UbE1L$^{-/-}$, neonatal mice were found to be more susceptible than wild-type (WT) mice to CHIKV-induced lethality, and yet no difference in viral burden was observed between ISG15$^{-/-}$, UbE1L$^{-/-}$, and WT mice (22). In addition, ISG15 was not found to affect CHIKV replication in tissue culture. Recent reports have also confirmed that extracellular free ISG15 can activate NK cells *in vitro* and augment the expression of gamma interferon in response to *Mycobacterium*, providing further evidence for an important biological role for free ISG15 during infection (34–36). These findings demonstrate that a more detailed characterization of the *in vivo* function of ISG15 during viral infection is warranted.

In this study we sought to determine whether inhibition of virus replication was a common mechanism by which ISG15 protects mice from respiratory virus infections. We found that both ISG15$^{-/-}$ and UbE1L$^{-/-}$ mice exhibited increased susceptibility to lethality induced by both influenza A virus and Sendai virus infections, demonstrating that this protection requires ISG15 conjugation. However, unlike what we have observed during influenza B virus infection, this protection did not appear to be mediated through the direct inhibition of virus replication. We also did not observe significant alterations in the cytokine response or the recruitment of inflammatory cells to the lungs after infection. Together, these results provide further evidence that ISG15 can protect the host from viral infection by mechanisms that extend beyond the regulation of viral replication.

MATERIALS AND METHODS

Mice. Mice were bred and maintained at Washington University School of Medicine in accordance with all federal and university guidelines, under specific-pathogen-free conditions. WT C57BL/6J mice were purchased from Jackson Laboratory (Bar Harbor, ME) and bred and maintained in our facilities. ISG15$^{-/-}$ mice (provided by Klaus-Peter Knobeloch, University Clinic Freiburg, Germany) and UbE1L$^{-/-}$ mice (provided by Dong-Er Zhang, University of California, San Diego, CA) were generated as previously described (37, 38). ISG15$^{-/-}$ and UbE1L$^{-/-}$ mice were fully backcrossed (>99.72 and 99.93%, respectively, to C57BL/6 by congenic SNP analysis through Taconic Laboratories (Hudson, NY).

Viruses. (i) Influenza A virus. Recombinant influenza A/WSN/33 (rWSN) virus was generated from cDNA as previously described (39). The virus was grown on MDCK cells using Dulbecco modified Eagle medium (DMEM) containing 1 μg/ml N-acetyltrypsin (Sigma Chemicals, St. Louis, MO), 100 U/ml penicillin, and 100 μg/ml streptomycin (Invitrogen, Carlsbad, CA). The cells were infected at a multiplicity of infection of 0.01 PFU/cell. Cell culture medium was harvested at 48 h postinfection and centrifuged to remove cell debris, and titers were determined by plaque assay in MDCK cells.

(ii) Influenza B virus. Recombinant WT influenza B/Yamagata/88 virus was grown in 10-day-old embryonated chicken eggs. Virus titers from allantoic fluid were determined by plaque assay in MDCK cells.

(iii) Sendai virus. Sendai/52 Fushimi strain virus was purchased from the American Type Culture Collection. Virus was plaque purified after infection of Vero cells to isolate a single clone that was then propagated in 11-day-old embryonated chicken eggs. Virus from allantoic fluid was diluted in phosphate-buffered saline (PBS) and stored at −80°C. Titers of viral stocks were determined by plaque assay in Vero cells.

Virus growth curves. Murine tracheal epithelial cultures were generated from the different genotypes of mice as previously described (40). Cells were harvested from the tracheas of female mice (5 to 12 weeks old) and grown under media in transwells (Corning) for 7 days. The apical medium was then removed, and the cells were grown at the air-liquid interface for 2 to 3 weeks prior to experimentation. For viral growth curves, virus was diluted in DMEM supplemented with 1% penicillin–1% streptomycin [DMEM(1%P/S)] to concentrations such that the indicated PFU were administered in volumes of 100 μl. Infections were performed by adding 100 μl of virus to the apical chamber and incubation at 37°C for 1 h. The virus was removed, and the apical chamber was washed three times with 200 μl of DMEM(1%P/S). After a washing step, 100 μl of DMEM(1%P/S) was added back to the apical chamber. At the indicated times, the apical medium was collected and replaced with 100 μl of DMEM(1%P/S). Virus titers in apical media were assessed by plaque assay on MDCK cells. For the beta interferon pretreatment conditions, beta interferon (PBL Assay Science) was added to basolateral media. After 24 h, immediately prior to infection, the basolateral media was removed, and the basolateral chambers were washed twice with PBS and then replaced with medium containing no interferon. The beta interferon doses and the viral infectious doses were different for each virus, as follows: influenza A virus, 50 U of beta interferon and 9×10^4 PFU; Sendai virus, 15 U of beta interferon and 9×10^5 PFU; and influenza B virus, 15 U of beta interferon β and 9×10^5 PFU.

***In vivo* infections.** Mice were anesthetized using an intraperitoneal injection of a ketamine-xyline cocktail prior to infection. For influenza A virus infections, 6- to 8-week-old female mice were intranasally (i.n.) infected with 5,000 PFU of influenza A/WSN/33 virus in 25 μl of PBS. For Sendai virus infections, 8- to 10-week-old male mice were infected i.n. with 1.2×10^6 PFU of Sendai virus in a total volume of 30 μl of PBS for Fig. 2 to 5. For the experiments performed in Fig. 6 to assess lung repair, mice were infected with a dose (0.6 to 1.0×10^6 PFU) that reduced lethality to ~20% in the infected ISG15$^{-/-}$ mice.

Lung viral load assessment. To assess lung titers, the right superior, middle, and inferior lobes were collected in 1 ml of PBS. Lungs were homogenized in a Roche MagNA Lyser using 1.0-mm-diameter zirconia/silica beads (BioSpec Products). The titers of lung homogenates were assessed by plaque assay using MDCK cells for influenza A virus and Vero cells for Sendai virus.

Infiltrating cell analysis. (i) Bronchoalveolar lavage analysis. Bronchoalveolar lavage fluid (BALF) was collected by inserting a catheter into the trachea and flushing 800 μl of PBS into and out of the lungs three times (~600 μl recovered). Lavages were centrifuged at a 2.5 relative centrifugal force for 5 min to pellet the cells. The supernatant was collected and analyzed for cytokines. Cells collected from lavages were resuspended in fluorescence-activated cell sorting (FACS) buffer (PBS, 3% bovine serum albumin, 0.1% sodium azide). BALF cells were counted by using a hemocytometer, and then cells from mice of the same genotype were pooled for further analysis. Red blood cells (RBCs) were lysed in 200 μl of RBC lysis buffer (Sigma) for 5 min at room temperature. The cells were washed in FACS buffer and incubated in FcR block for 30 min. The cells were then stained in different mixes of antibodies against cell surface markers for 30 min, washed three times in FACS buffer, fixed in 1% formaldehyde, and analyzed by flow cytometry (BD FACSCanto).

(ii) Lung homogenates. To analyze infiltrating cells in the lung parenchyma, the left lung was collected from a lavaged mouse. The lung was minced with scissors and incubated in DMEM with 350 U/ml collagenase type I (Worthington) and 50 U/ml DNase (Worthington) for 1 h at 37°C. The remaining tissue after enzymatic digestion was crushed between the rough edge of a frosted microscope slide. The cells were passed through a cell strainer. RBCs were lysed in 1 ml of RBC lysis buffer (Sigma) for 5 min at room temperature. The cells were then washed with FACS buffer, blocked, stained, and analyzed as described above for BALF cells.

Total lung and lavage cell counts were determined by counting cells that excluded trypan blue using a hemocytometer. The cell count data for each time point were collected from infected WT mice (6 to 9 mice, collected from 3 to 4 independent infections), ISG15$^{-/-}$ mice (6 to 8 mice, collected from 3 to 4 independent infections), and UbE1L$^{-/-}$ mice (5 to 8 mice, collected from 2 to 3 independent infections). Cell counts from mock-infected lungs (2 mice per genotype collected from 2 independent experiments) and BALF (5 to 6 mice collected from 5 independent experiments) were pooled from various times after mock infection since cell counts did not differ between days after mock infection.

Data in flow cytometry analysis of cell types represent a total of 6 to 8 mice collected from 3 independent experiments for WT and ISG15$^{-/-}$ mice, and 5 to 8 total mice collected from 2 to 3 experiments for UbE1L$^{-/-}$ mice, per time point. Cell populations were defined as follows: neutrophils (Cd11b^{+} Ly6G^{+} MHCII^{-}), Inflammatory monocytes (Cd11b^{+} Ly6G^{-} Ly6C^{int} MHC-II^{int} Cd11c^{int}), NK cells (CD3^{-} NK1.1^{+}), CD8^{+} T cells (CD3^{+} CD8^{+}), CD4^{+} T cells (CD3^{+} CD4^{+}), and B cells (CD19^{+}).

Antibodies. The following antibodies were purchased from eBioscience: fluorescein isothiocyanate (FITC)-conjugated anti-MHC-II (M5/114.15.2), allophycocyanin-conjugated (APC) anti-B220 (RA3-682), PERCP-Cy5.5 anti-CD11b (M1/70), and PERCP-Cy5.5 anti-CD3ε (145-2C11). The following antibodies were purchased from BioLegend: FITC-conjugated anti-CD8 (53-6.7), phycoerythrin (PE)-conjugated anti-Ly6G (1A8), PE-conjugated anti-CD19 (6D5), APC-conjugated anti-CD11c (N418), and Pacific Blue-conjugated anti-Ly6c (HK1.4). The following antibodies were purchased from BD Biosciences: PE-conjugated anti-CD4 (GK1.5) and APC-conjugated anti-NK1.1 (PK136).

Cytokine analysis. BALF was collected as described above and analyzed using Bio-Rad Bio-Plex analysis according to the manufacturer's instructions. Quantification of alpha interferon in BALF was performed using a pan-alpha-interferon enzyme-linked immunosorbent assay (ELISA; PBL Assay Science).

Sendai virus. Data from all time points were generated from 6 to 8 mice collected from 3 separate infections, except for the UbE1L$^{-/-}$ day 3 data, which were generated from 5 mice from 2 infections. Cytokine analysis of mock-infected mice was generated from 2 mice of each genotype for days 3 and 6 after mock infection (intranasal PBS instillation), and one mouse from each genotype for day 8 after mock infection. Analytes in mock-infected BALF did not vary between genotype or day after mock infection; thus, all mock values were pooled.

Influenza A virus. WT and ISG15$^{-/-}$ data were generated from 5 to 6 mice from 1 to 2 experiments per time point. UbE1L$^{-/-}$ data were generated from 3 to 4 mice from one experiment per time point. Mock infection data were generated from 4 to 6 mice from 2 to 3 experiments per time point. No differences were detected between any genotype at any time points; thus, all mock values were pooled.

Histology. For lung histological analysis, mice were infected as described above and sacrificed at the indicated times postinfection. Either the left lobe was inflated with 500 μl of formalin or all lobes were inflated with 1.0 ml of formalin. Lungs were removed and incubated in a 50-ml conical tube containing 15 ml of formalin. After 36 to 48 h in formalin, lungs were washed for 15 min in serial washes using PBS, 30% ethanol, and 50% ethanol and then stored in 70% ethanol until they were processed for paraffin embedding, sectioning, and staining. Lung sections were stained with hematoxylin and eosin and scored blindly by a pathologist (T.S.S.). An average of 52.8 small airways (100 to 300 μm in diameter) were scored per mouse (range, 33 to 89; median, 46).

Statistics. All data were analyzed using Prism software (GraphPad, San Diego, CA). Statistical analyses used for particular experiments are indicated in figure legends. Error bars in all figures represent the standard errors of the mean.

RESULTS

ISG15 functions in a conjugation-dependent manner to protect mice from influenza A virus-induced lethality without altering viral loads. We previously showed that ISG15 contributes to the host response against both influenza A virus and influenza B virus, since ISG15$^{-/-}$ mice exhibit increased lethality after infection compared to WT mice (21). ISG15-mediated protection against influenza B virus infection is dependent upon ISG15 conjugation and results in a dramatic reduction in viral loads *in vivo* (24). To determine whether the protective activity of ISG15 during influenza A virus infection was also dependent upon conjugation, we infected WT, ISG15$^{-/-}$, and UbE1L$^{-/-}$ mice with 5.0×10^3 PFU of influenza A/WSN/33 virus i.n. and monitored the mice for lethality. As expected, ISG15$^{-/-}$ mice displayed increased lethality compared to WT mice (Fig. 1A). This protection mediated by ISG15 appeared to be largely conjugation dependent, since UbE1L$^{-/-}$ mice also displayed increased lethality compared to WT mice (Fig. 1A). Interestingly, despite the large difference in survival, the extent of weight loss in both ISG15$^{-/-}$ and UbE1L$^{-/-}$ mice was similar to the weight loss observed in WT mice through 9 days postinfection, after which both ISG15$^{-/-}$ and UbE1L$^{-/-}$ mice began to succumb to infection (Fig. 1B). This observation is strikingly different from what we previously reported for influenza B virus infection, where increased mortality in both ISG15$^{-/-}$ and UbE1L$^{-/-}$ mice was associated with a dramatic increase in weight loss compared to WT mice (24).

The increased lethality we previously observed in ISG15$^{-/-}$ mice during influenza B virus infection was also accompanied by a 2- to 3-log increase in virus titers at days 3 and 6 postinfection compared to WT mice (24). To determine whether ISG15 played a similar role during influenza A virus infection, we next evaluated viral loads within the lungs of infected mice during the course of infection. Virus could be detected in the lung 1 day postinfection, with all three genotypes of mice displaying similar virus titers

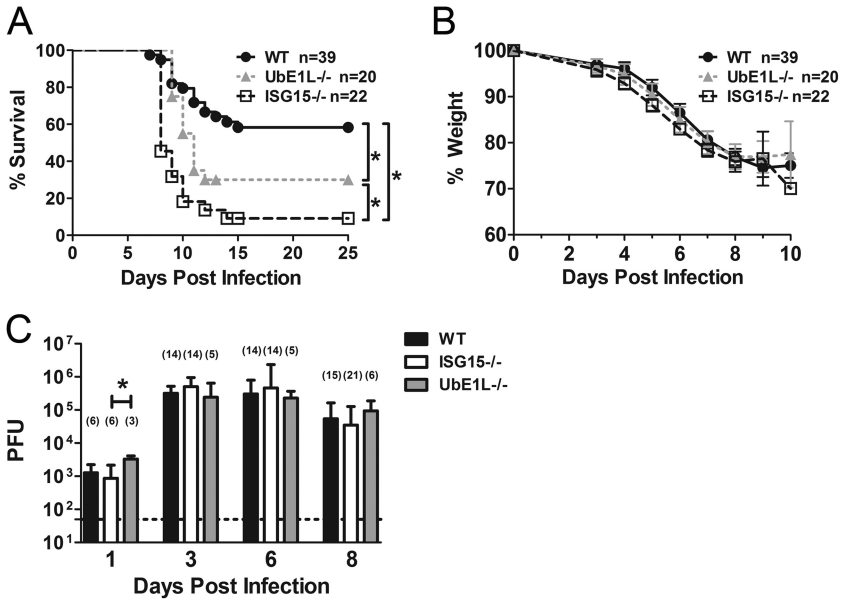

FIG 1 ISG15 protection against influenza A virus is conjugation dependent but not antiviral. WT, ISG15$^{-/-}$, and UBE1L$^{-/-}$ mice were infected with 5.0×10^3 PFU of influenza A/WSN/33 i.n. Mice were monitored for lethality (A) and weight loss (B), or they were sacrificed at the indicated times postinfection, and viral loads in the lungs were assessed by plaque assay (C). For vial load assessment, the numbers of mice analyzed per genotype at each time point are indicated in parentheses. Lung titer samples were collected from 1 to 6 independent experiments. Panel A: *, $P < 0.05$, Mantel-Cox test. Panel B: *, $P < 0.05$, Kruskal-Wallis, followed by Dunn's posttest was performed for each time point.

(Fig. 1C). Peak virus titers were reached by 3 days postinfection, but despite the increased lethality observed in both ISG15$^{-/-}$ and UbE1L$^{-/-}$ mice, we observed similar viral loads in all mice at both days 3 and 6 postinfection. On day 8 postinfection the lung titers were still similar between the three genotypes as the mice began to clear the virus. Staining lung sections with an anti-influenza A virus polyclonal serum revealed a similar pattern of staining and clearance of the bronchiolar and alveolar epithelium in both WT and ISG15$^{-/-}$ mice (data not shown). These results suggest that during influenza A virus infection ISG15 protects the host from lethality in a conjugation-dependent manner that is independent of its previously reported effects on viral replication.

ISG15 also protects mice from Sendai virus induced lethality in a conjugation-dependent manner with minimal impact upon viral loads. We next wanted to determine whether increased lethality in ISG15$^{-/-}$ mice without a concomitant increase in viral load was unique to influenza A virus infection. We chose to evaluate the pathogenesis of Sendai virus (a mouse paramyxovirus) in ISG15$^{-/-}$ mice, since it is a natural mouse pathogen. We infected WT, ISG15$^{-/-}$, and UbE1L$^{-/-}$ mice i.n. with 1.2×10^6 PFU of Sendai virus and monitored the animals for weight loss and lethality. We found that ISG15 protected mice from Sendai virus-induced lethality in a conjugation-dependent manner. In WT mice, infection induced significant disease with a ca. 25% weight loss but was rarely lethal (Fig. 2A and B). In contrast, nearly 70% of the ISG15$^{-/-}$ and UbE1L$^{-/-}$ mice succumbed to infection by day 10 postinfection despite exhibiting weight loss similar to that of WT controls (Fig. 2B). We next evaluated viral loads in the lungs of these mice during the course of Sendai virus infection. Once again, unlike the 2- to 3-log increases in viral replication that we observed during influenza B virus infection, we noted minimal differences in viral loads between the three genotypes during the course of Sendai virus infection. In all three genotypes of mice, peak viral loads were reached at 3 days postinfection, with no differences noted between the genotypes (Fig. 2C). At 6 days postinfection there was a small, ~3-fold, increase in viral loads in the ISG15$^{-/-}$ and UbE1L$^{-/-}$ mice compared to WT mice. By day 8 postinfection, all three genotypes of mice had started to clear the virus, and we observed no difference in viral loads between WT and ISG15$^{-/-}$ mice, although we did detect increased viral burdens in the UbE1L$^{-/-}$ mice. Staining for viral antigen using an anti-Sendai virus polyclonal serum revealed no differences in viral spread during the course of infection between WT and ISG15$^{-/-}$ mice (data not shown). Thus, ISG15 protected mice from Sendai virus-induced lethality in a conjugation-dependent manner while having only a minimal impact upon viral burden over the course of the infection.

ISG15 does not affect influenza A virus or Sendai virus replication *in vitro*. Although we did not observe a major difference between influenza A virus or Sendai virus burden in ISG15$^{-/-}$ and WT mice, it has been previously reported that ISG15 conjugation can antagonize both influenza A virus and Sendai virus replication in human cell lines. Small interfering RNA (siRNA) knockdown of ISG15 or HERC5 in HEK293 cells resulted in increased Sendai virus replication (28). Similarly, siRNA knockdown of ISG15 or HERC5 in A549 cells or ISG15 and UbE1L in Calu3 cells resulted in ca. 5- to 10-fold increases in influenza A virus replication (25, 27). Given these previous findings, and the fact that we did see a small increase in Sendai virus titers in ISG15$^{-/-}$ mice at day 6 postinfection, we wanted to more carefully evaluate whether ISG15 can directly impact viral replication in the mouse model. To this end, we generated primary murine trachea epithelial cells (mTECs) from WT, ISG15$^{-/-}$, and UbE1L$^{-/-}$ mice and evaluated influenza A virus and Sendai virus growth in these cells.

First, we infected mTECs with influenza B virus to determine whether these cultures could recapitulate the increase in virus rep-

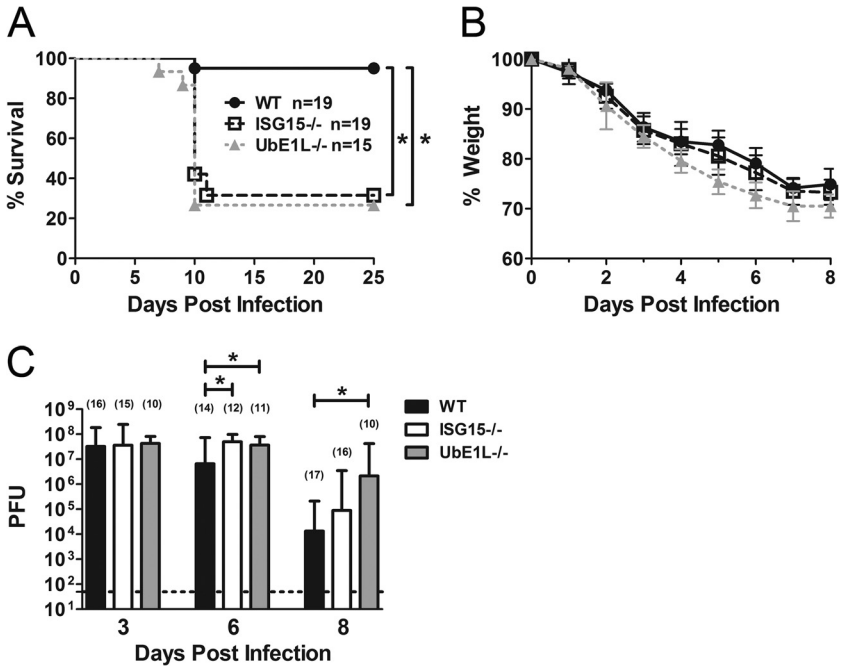

FIG 2 ISG15 protects against Sendai virus induced lethality by a conjugation-dependent mechanism but has no major effect on virus loads. WT, ISG15$^{-/-}$, and UBE1L$^{-/-}$ mice were infected with 1.2×10^6 PFU of Sendai virus i.n. and monitored for (A) lethality and (B) weight loss, or were sacrificed at the indicated times postinfection and viral loads in the lungs were assessed by plaque assay (C). For vial load assessment, the numbers of mice analyzed per genotype at each time point are indicated in parentheses. Lung titer samples were collected from 2 to 6 experiments. Weight loss data were compiled from 7 to 11 independent infections of mice, some of which were sacrificed prior to day 8. The data are composed of 28 to 45 mice per genotype through day 6, 23 to 37 mice per genotype through day 8. Panel A: *, $P < 0.05$, Mantel-Cox test. Panel C: *, $P < 0.05$, Kruskal-Wallis test, followed by Dunn's posttest was performed for each time point.

lication observed *in vivo* in ISG15$^{-/-}$ mice. In cultures that were not pretreated with interferon, a small but statistically significant increase in influenza B virus replication was observed at late time points in mTECs derived from ISG15$^{-/-}$ mice (Fig. 3A). The pretreatment of cultures with beta interferon for 24 h prior to infection, in order to induce ISG15 expression and conjugation, resulted in a 33-fold increase in replication in the ISG15$^{-/-}$ cells (Fig. 3B). Next, we assessed the replication of influenza A virus and Sendai virus in mTECs lacking ISG15 or UbE1L. In untreated mTECs both influenza A virus and Sendai virus grew with similar kinetics in WT, ISG15$^{-/-}$, and UbE1L$^{-/-}$ cells (Fig. 3C and E). We then pretreated the mTEC cultures with a dose of beta interferon that induced ISG15 conjugation and resulted in ~100-fold inhibition of virus replication in WT mTECs at 24 to 36 h postinfection. However, even after interferon stimulation we observed no difference in the replication of either influenza A virus or Sendai virus in any of the three genotypes of mTECs (Fig. 3D and F). These results, together with our *in vivo* virus titer data, suggest that during both influenza A virus and Sendai virus infection ISG15 does not directly inhibit virus replication within infected cells and therefore appears to protect the host from lethality by a mechanism that is distinct from its role during influenza B virus infection.

The loss of ISG15 does not alter the cytokine response during influenza A virus or Sendai virus infection. We have recently reported that increased lethality in ISG15$^{-/-}$ mice after CHIKV infection results from a cytokine storm and not from an inability to control virus replication (22). We therefore wanted to evaluate whether ISG15 regulation of the cytokine response to infection might be responsible for the increased lethality in ISG15$^{-/-}$ mice after influenza A virus or Sendai virus infection.

We infected WT, ISG15$^{-/-}$, and UbE1L$^{-/-}$ mice with influenza A virus and at days 3, 6, and 8 postinfection mice were sacrificed to collect BALF. We then evaluated a panel of 10 proinflammatory cytokines in the BALF. The levels of all cytokines evaluated peaked at 6 days postinfection and were either not detectable or were greatly reduced by day 8 postinfection (Fig. 4A). We observed very few statistically significant differences in cytokine levels. Importantly, for the two cytokines that we did observe differences (IL-6 and RANTES), these differences were not consistently seen in ISG15$^{-/-}$ and UbE1L$^{-/-}$ mice.

We performed a similar analysis of BALF cytokines during Sendai virus infection. Once again, all cytokines analyzed were induced above mock infection levels in all three genotypes of mice (Fig. 4B). Similar to what we observed during influenza A virus infection, no dramatic differences were observed in the overall BALF cytokine response between WT, ISG15$^{-/-}$, or UbE1L$^{-/-}$ mice after Sendai virus infection, and any differences that were seen were not consistent between ISG15$^{-/-}$and UbE1L$^{-/-}$ mice (Fig. 4B).

Finally, we evaluated using ELISA the alpha interferon levels in BALF from Sendai virus-infected mice. We observed no difference in alpha interferon production in WT, ISG15$^{-/-}$, or UbE1L$^{-/-}$ mice at any time after Sendai virus infection (Fig. 4C). Total alpha interferon levels peaked at 3 days postinfection, similar to the virus titers in the lungs, and diminished over the course of infection. Overall, the ISG15$^{-/-}$ and UbE1L$^{-/-}$ mice appear to produce a normal interferon and cytokine response during both influenza A virus and Sendai virus infection, unlike the global cytokine misregulation observed in ISG15$^{-/-}$ mice during CHIKV infection (22).

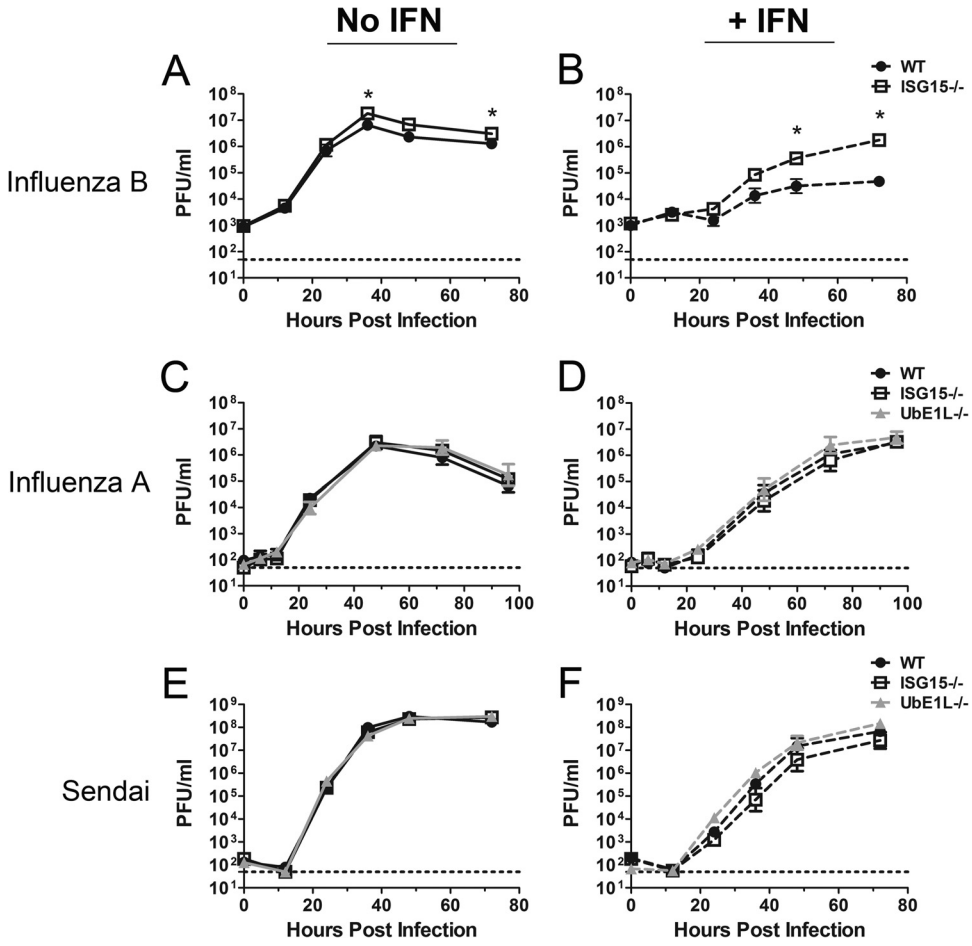

FIG 3 Influenza A virus and Sendai virus replication is not altered in primary tracheal epithelial cultures lacking ISG15 or ISG15 conjugates. Primary murine trachea epithelial cell cultures were generated from WT, ISG15$^{-/-}$, and UBE1L$^{-/-}$ mice. Cultures were either left unstimulated (A, C, and E) or stimulated with beta interferon for 24 h (B, D, and F) before infection with influenza B/Yamagata/88 (A and B), influenza A/WSN/33 (C and D), or Sendai (E and F)virus. Titers were determined by plaque assay in apical medium at various times after infection to evaluate virus replication. Virus growth curves were generated from two infections performed on different mTEC preparations with a total of 5 to 6 total replicates between the two infections. Panels A and B: *, $P < 0.05$, Mann-Whitney test. Panels C to F: *, $P < 0.05$, Kruskal-Wallis test, followed by Dunn's posttest.

Similar immune cell populations are recruited to the lungs in WT, ISG15$^{-/-}$, and UbE1L$^{-/-}$ mice during Sendai virus infection. Much of the tissue damage incurred after respiratory virus infection is believed to be a result of immunopathology induced in response to the virus (41, 42). Although neutrophils and inflammatory macrophages are necessary for the control of virus replication, it is thought that excessive recruitment of these cell types can lead to excessive damage of the lung resulting in mortality (43–46). We therefore next evaluated the cellular recruitment to the lungs of ISG15$^{-/-}$ mice during Sendai virus and influenza A virus infections.

An analysis of gross lung histopathology from infected mice revealed no obvious difference in the degree of inflammation between all three genotypes of mice after either influenza A virus or Sendai virus infection (data not shown). To evaluate this quantitatively, we infected mice with Sendai virus and, at various times postinfection, we analyzed the total number of cells recovered from lung parenchyma digests and BALF. We observed no major differences in the total number of cells collected from the lung parenchyma or BALF of WT, ISG15$^{-/-}$, or UBE1L$^{-/-}$ mice after infection (Fig. 5A and B). We also observed no difference in total cell numbers recruited to the lungs of WT and ISG15$^{-/-}$ mice after influenza A virus infection (data not shown).

We next analyzed the types of cells recruited to the lung during Sendai virus infection by performing flow cytometric analysis on cells isolated from lung parenchyma digests. We found an elevation of neutrophils, inflammatory monocytes, and NK cells over mock-infected levels by day 3 postinfection in all strains. However, there were no significant differences observed between WT, ISG15$^{-/-}$, or UbE1L$^{-/-}$ mice at 3 or 6 days postinfection (Fig. 5C). The only difference we observed was a 2-fold increase in inflammatory monocytes in ISG15$^{-/-}$ lungs compared to WT mice at day 8 p.i. We observed T-cell recruitment above mock-infected levels starting at day 6 postinfection, but we observed no differences in CD8^{+} or CD4^{+} T-cell numbers between genotypes (Fig. 5D). We also observed similar percentages of cell types recovered from BALF from WT, ISG15$^{-/-}$, and UbE1L$^{-/-}$ mice infected with Sendai virus (data not shown). Based on these findings, we observed no major differences between the three strains of mice in either

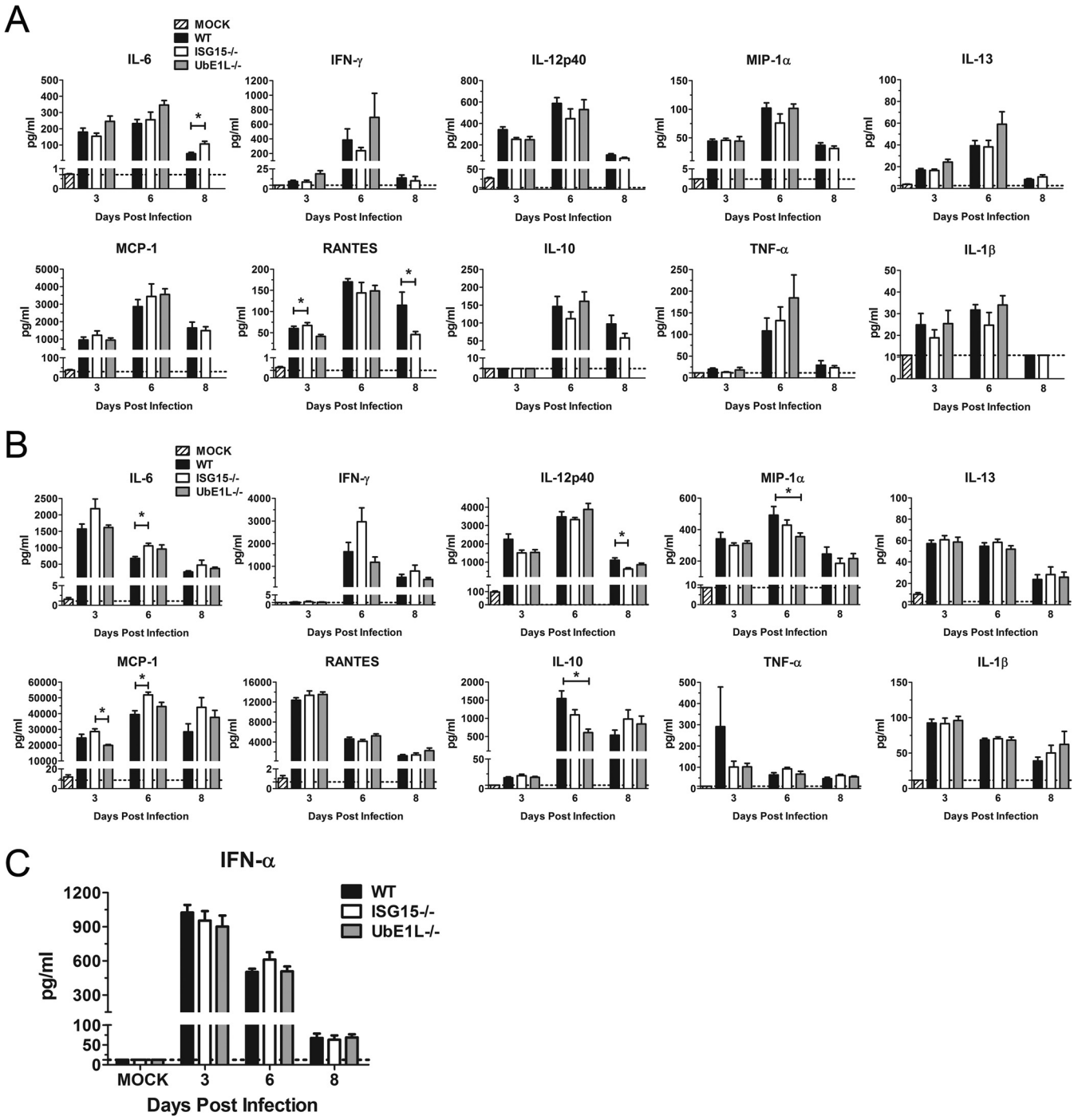

FIG 4 ISG15 does not affect cytokine production after influenza A virus or Sendai virus infection. WT, ISG15$^{-/-}$, and UBE1L$^{-/-}$ mice were infected with 5.0×10^3 PFU of influenza A/WSN/33 virus (A) or 1.2×10^6 PFU of Sendai virus (B) i.n. At days 3, 6, and 8 postinfection, mice were sacrificed and BALF was analyzed for cytokines and chemokines by Bio-Rad multiplex analysis. (C) BALF from Sendai virus-infected mice was analyzed for the levels of alpha interferon by ELISA. Panels A to C: *, $P < 0.05$, Kruskal-Wallis test, followed by Dunn's posttest, was performed for each time point except for day 8 (panel A), for which a Mann-Whitney test was used.

the number or the composition of inflammatory cells recruited to the lung after infection.

During recovery from infection mice lacking ISG15 display an increase in diseased airways. Although previous studies of respiratory virus pathogenesis have revealed that immunodeficiency can lead to the spread of virus outside the lung, we were unable to detect either influenza A virus or Sendai virus by plaque assay in the kidney, spleen, liver, heart, or brain at day 8 postinfection (data not shown) (47). Histological analysis of these organs revealed no pathology outside the lung (data not shown). A

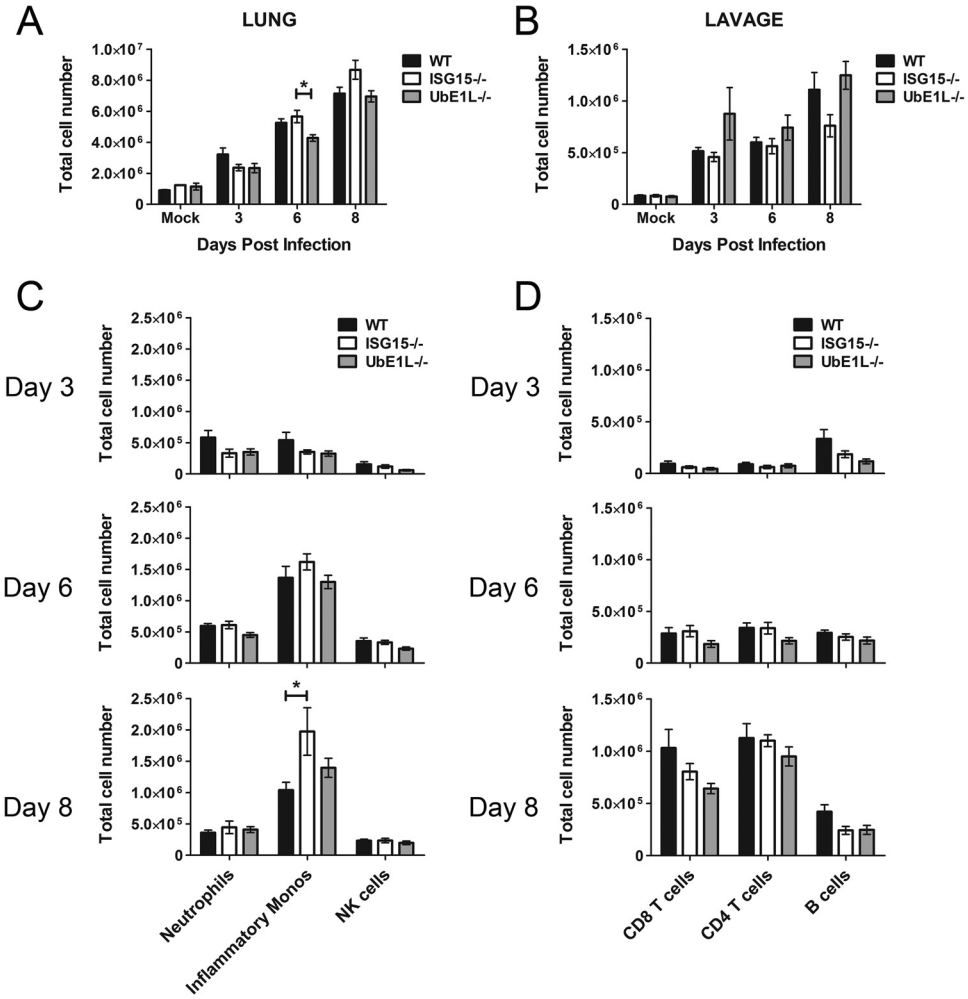

FIG 5 Similar numbers and cell populations are recruited to the lungs during Sendai virus infection in the presence or absence of ISG15 conjugation. WT, ISG15$^{-/-}$, and UBE1L$^{-/-}$ mice were infected with 1.2×10^6 PFU of Sendai virus i.n. At days 3, 6, and 8 postinfection, mice were sacrificed, and the lungs were lavaged and subsequently processed into single cell suspensions. Single cell suspensions of digested lungs (A) and cells from the lavage (B) were analyzed for total cell number based on hemocytometer counting. (C and D) Cell populations recovered from lung digests were stained for cell surface markers and analyzed by FACS as described in Materials and Methods. *, $P < 0.05$, Kruskal-Wallis test, followed by Dunn's posttest.

careful histological evaluation of the lung epithelium at day 8 postinfection revealed similar damage in both ISG15$^{-/-}$ and UbE1L$^{-/-}$ mice compared to WT mice (data not shown). We noted that during both influenza A virus and Sendai virus infection the ISG15$^{-/-}$ and UbE1L$^{-/-}$ mice succumb to infection at around days 9 to 10 postinfection (Fig. 1 and 2). Previous characterization of the lung histopathology during influenza A virus and Sendai virus infection have shown that at this time the airway epithelium is beginning to repair itself from the damage induced during the infection (48–50). We therefore hypothesized that ISG15 may play a role in lung repair after infection.

In order to evaluate the lung pathology during this healing phase, we decreased the infectious dose of Sendai virus so that only 20% of ISG15$^{-/-}$ and UbE1L$^{-/-}$ mice succumbed to infection (Fig. 6A). Interestingly, at this lower dose, while WT mice began to regain body weight at day 8 postinfection, the ISG15$^{-/-}$ and UbE1L$^{-/-}$ mice were delayed in initiating weight recovery (Fig. 6B). At day 11 postinfection both ISG15$^{-/-}$ and UbE1L$^{-/-}$ mice had recovered only 75% of their initial body weight compared to the 85% weight recovery observed in the WT mice. An analysis of viral loads in the lungs revealed that, similar to the higher dose of infection, peak virus titers were observed at days 3 and 6 postinfection in all genotypes, and by day 11 postinfection all three genotypes of mice had cleared replicating virus (Fig. 6C). At day 3 postinfection, we did note a small increase in viral loads (~3-fold) in ISG15$^{-/-}$ mice compared to WT mice. Histological evaluation of lungs harvested from these mice at day 11 postinfection showed increased numbers of abnormal small terminal airways in the ISG15$^{-/-}$ mice compared to WT mice (Fig. 5D to H). These abnormal airways were either in the form of denuded airways (no epithelial cells present) or extensive epithelial proliferation that spills over into adjacent alveoli. Therefore, during recovery from Sendai virus infection mice lacking ISG15 displayed an increase in diseased airways.

DISCUSSION

Due to its robust expression after type I interferon stimulation, ISG15 has long been hypothesized to contribute to the interferon-

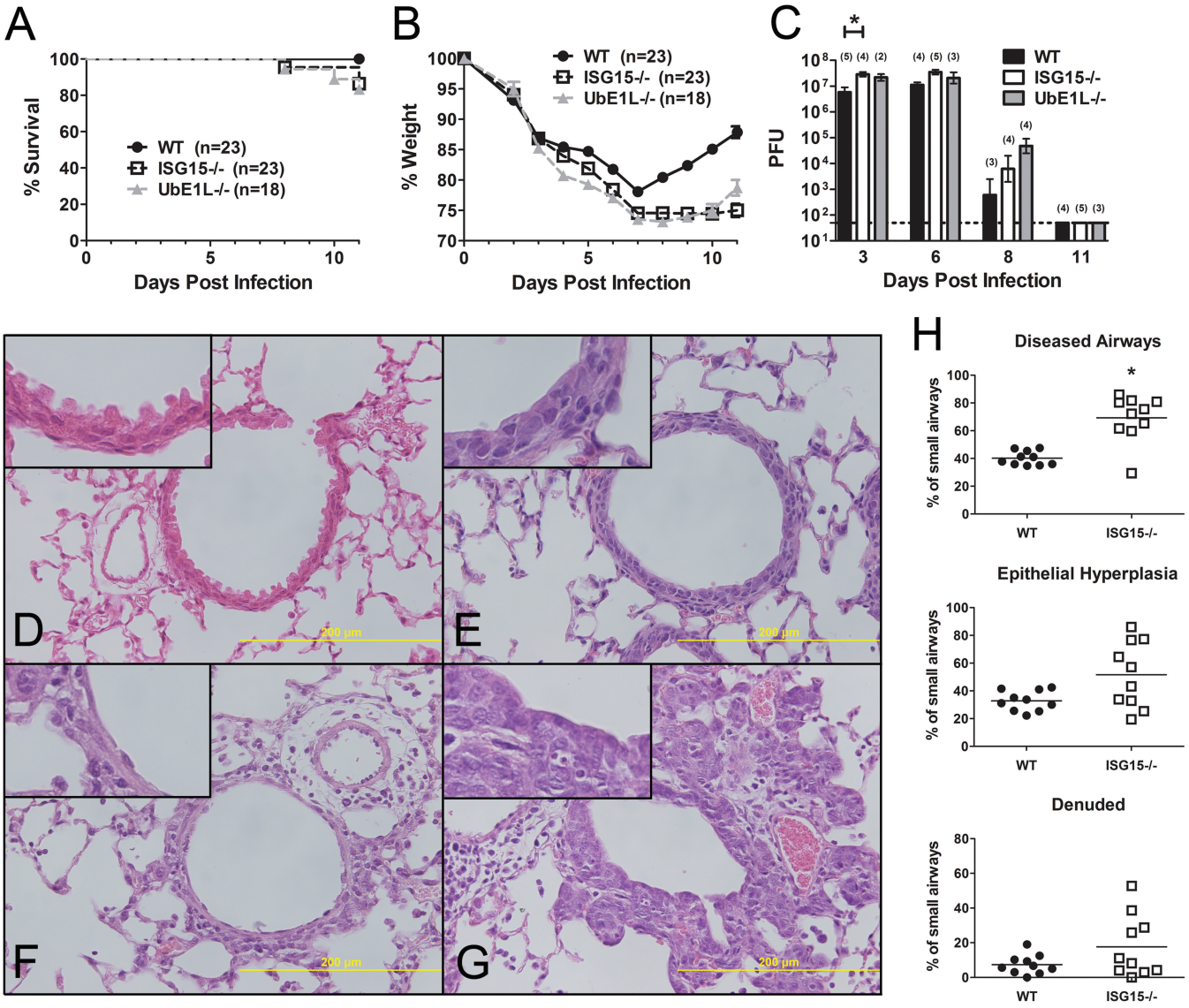

FIG 6 Infection with Sendai virus at a lower dose reveals increased weight loss and distal airway damage in ISG15$^{-/-}$ mice. WT, ISG15$^{-/-}$, and UbE1L$^{-/-}$ mice were infected with 0.6×10^6 to 1.0×10^6 PFU of Sendai virus and were monitored for lethality (A) and weight loss (B). (C) Viral loads in the lungs of mice were analyzed at days 3, 6, 8, and 11 days postinfection by plaque assay. (D to H) Lungs from mice infected with Sendai virus were harvested at 11 days postinfection, fixed, sectioned, and stained with hematoxylin and eosin. (D) Representative image of a small airway from a mock-infected mouse. (E to G) Representative images of small airways from a mouse 11 days after Sendai virus infection exhibiting no aberrant disease (E), denudation of epithelium (F), or epithelial hyperplasia (G). The insets represent an expanded view of a section of epithelium. (H) Stained sections were scored blindly by a pathologist for evidence of damage to the small terminal airways, including epithelial hyperplasia and denuded airways. Panel C: *, $P < 0.05$, Kruskal-Wallis test, followed by Dunn's posttest. Panel H: *, $P < 0.05$, Mann-Whitney test.

mediated intracellular antiviral response. Supporting this hypothesis, ISG15$^{-/-}$ mice are more susceptible than WT mice to certain viral infections, and a number of reports have been published showing the ability of ISG15 to antagonize replication of viruses in tissue culture. One way that this inhibition has been shown to occur is through the ISGylation of viral and host proteins. ISGylation of human papillomavirus capsid protein has been shown to inhibit the infectivity of virus that incorporates ISGylated capsid, and ISGylation of the influenza A virus NS1 protein has been shown both to inhibit its ability to associate with importin α and to affect its ability to antagonize the interferon response (26, 27, 29). In addition, hundreds of host proteins are also ISGylated, and these modifications likely contribute to antagonizing the virus life cycle. In the case of Ebola virus, ISG15 can inhibit virus-like particle release by inhibiting the ubiquitin E3 ligase activity of Nedd4 (32, 33). These examples demonstrate the diversity of mechanisms by which ISG15 can inhibit virus replication.

Although there is now evidence that ISG15 can act as a protective factor during CHIKV infection by a mechanism that does not involve inhibition of virus replication, this observation was found to be mediated by the unconjugated form of ISG15 (22). We report here a novel mode of ISG15-mediated protection from virus infection. We have shown that similar to its role during influenza B virus infection, ISG15 protects mice from influenza A virus in a

conjugation-dependent manner. However, while ISG15 is important for protecting mice from influenza A virus-induced lethality, we observed no difference in virus burden, suggesting that ISG15 protects mice from influenza A virus and influenza B virus by two distinct mechanisms. Moreover, unlike its role during CHIKV infection, ISG15 had no effect on cytokine regulation after influenza A virus infection. We have also shown that this mode of ISG15-mediated protection does not appear to be unique to influenza A virus infection. Through the evaluation of Sendai virus pathogenesis in ISG15$^{-/-}$ and UbE1L$^{-/-}$ mice, we found that ISG15 conjugation protects mice from Sendai virus by a mechanism that closely resembles the characteristics of ISG15-mediated protection against influenza A virus infection.

In these two models ISGylation appears to have minimal impact upon viral replication *in vitro* or *in vivo*. In the Sendai virus model, while we did detect a small increase in viral loads in ISG15$^{-/-}$ and UbE1L$^{-/-}$ mice compared to WT mice at certain times, these differences paled in comparison to the magnitude by which ISG15 restricts influenza B virus replication (24). In addition, we observed no difference in influenza A virus or Sendai virus replication in mTECs. It has previously been reported that ISG15 inhibits the replication of both influenza A virus and Sendai virus in tissue culture (25–28). The discrepancies between our findings and previously published data could reflect a difference between a primary heterogeneous culture of cells and immortalized cell lines. There is precedent for cell type specific effects of ISG15 on influenza A virus replication, which is now further supported by the fact that we did not initially detect a difference in influenza B virus replication in ISG15$^{-/-}$ embryonic fibroblasts (21, 25). It is also possible that these discrepancies reflect a difference in the function or specificity of human and murine ISG15. Such species specificity has been reported with respect to the influenza B virus NS1 protein (B/NS1), which can bind to and inhibit conjugation of human and primate ISG15 but not mouse ISG15 (51, 52). Further studies will be needed to explain these discrepancies.

Previously it was shown that influenza A virus NS1 protein is ISGylated in A549 cells. In this system, this modification accounted for most of the antiviral activity of ISG15 against influenza A virus (26, 27). One potential explanation for ISG15 not affecting influenza A virus or Sendai virus replication in our system is that viral proteins are not being ISGylated. We have found that expression of the murine ISG15 conjugation system and influenza virus proteins in 293T cells can result in the ISGylation of viral proteins (data not shown). However, we do not know whether these proteins are also modified in the respiratory epithelium during the course of infection. If influenza A virus or Sendai virus proteins are modified during infection, our data would suggest that these modifications do not have a significant effect on replication. However, such modifications could still play a role during pathogenesis *in vivo* through the regulation of other host responses such as cell death or antigen presentation. This important line of research could shed more light on additional mechanisms by which ISG15 regulates pathogenesis.

A surprising observation from these studies is the differential effects that ISG15 has on influenza A and influenza B virus replication. However, this finding is not entirely unexpected. The function of ISG15 conjugation during influenza A virus and influenza B virus infection *in vivo* correlates with the effects of type I interferons on these viruses *in vivo*. IFNAR$^{-/-}$ mice display dramatically elevated viral loads compared to WT mice during influenza B virus infection (24). Whereas a number of studies have found either no difference or only small differences in virus replication and virus clearance in IFNAR$^{-/-}$ mice during influenza A virus or Sendai virus infection (53–56). As mediators of the interferon response, ISGs might then also be expected to have different effects on influenza A virus compared to influenza B virus. In addition, studies of the NS1 protein of influenza A and B viruses have suggested that ISG15 might play distinct roles during these infections. B/NS1 binds to human and primate ISG15, resulting in the inhibition of ISG15 conjugate formation (52). Influenza A/NS1 virus does not bind to ISG15; however, unlike B/NS1, A/NS1 has a greater capacity to inhibit the interferon response and the induction of ISGs, including ISG15, in infected cells (51). This suggests either that ISG15 has imposed a different evolutionary pressure on influenza B virus compared to influenza A virus or that influenza A virus has adapted to the evolutionary pressure of ISG15 through an alternative mechanism.

There could be a number of reasons to explain the differential effect of ISG15 on influenza A and B viral infection. As noted previously, these viruses may have differential sensitivity to the effects of IFNs due to the immune evasion strategies that they employ. In addition, influenza A and B viruses may use distinct cellular pathways during their replication cycles which can be differently regulated by ISG15. Finally, it is interesting that a comparison of the lysine content of influenza A/WS/1933, A/PR8/1934, and A/California/2009 viruses to that of influenza B/Lee/1940, B/Yamagata/1988, and B/Victoria/1987 viruses reveals that the influenza B virus proteome contains an ~35% increase in total lysine residues compared to influenza A virus. It is tempting to speculate that this might render influenza B virus more susceptible to potentially detrimental effects of viral protein ISGylation. Further research into influenza B virus biology will be needed in order to explain these differences in the effects of ISG15 and interferon on the pathogenesis of influenza A and influenza B viruses.

In both influenza A virus- and Sendai virus-infected mice we observed lethality at around 9 to 10 days postinfection, a time when mice are clearing the acute viral infection, beginning to regain weight, and beginning to repair the airway epithelium. By lowering the infectious dose of virus and allowing a significant number of the ISG15$^{-/-}$ mice to survive infection, we observed a difference in the ability of the ISG15$^{-/-}$ mice to recover weight, and histological examination of the lungs revealed increased disease in the smaller airways of the lung in the ISG15$^{-/-}$ mice. These histological changes noted in the airway epithelium are consistent with previous reports of Sendai virus pathogenesis (57, 58). One study evaluating the disease susceptibility of different mouse strains to Sendai virus found that although resistant and susceptible mouse strains have dramatically different 50% lethal dose titers, little difference in viral loads or viral clearance was observed between mouse strains over the course of infection (58). The increased susceptibility to Sendai virus induced lethality appeared to correlate with an increase in the number of airways exhibiting delayed re-epithelialization or epithelial hyperplasia.

It is not clear whether the increase in diseased airways we observed in ISG15$^{-/-}$ mice during Sendai virus infection is a result of increased damage, a defect in the wound repair response, or some combination of both. Different functions that have been previously described for ISG15 could support a role for ISG15 in

either process. It has been shown that ISG15 inhibits apoptosis through ISGylation of filamin B and that ISG15$^{-/-}$ peritoneal macrophages have a reduced phagocytic capacity (59, 60). Either increased apoptosis or a decreased capacity to clear apoptotic bodies might result in increased damage in the distal airways of ISG15$^{-/-}$ mice. A number of viruses have been reported to induce apoptosis, and it is thought that in some cases this might facilitate virus spread (61). Thus, an inability to control apoptosis or clear apoptotic debris might also account for the small differences in viral load observed in ISG15$^{-/-}$ mice during Sendai virus infection *in vivo*.

Bronchial epithelial healing after Sendai virus infection involves the loss of epithelial differentiation markers on cells after infection, cell proliferation and migration to repopulate the damaged airways, and differentiation of cells into the proper epithelial cell types (48). Although it is unclear whether ISG15 plays a role in these processes, one study has shown that the knockdown of ISG15 or UbCH8 in a breast cancer cell line resulted in a reorganization of the actin cytoskeleton and the decreased ability of a cell monolayer to close a scratch wound in tissue culture (62). Therefore, it is possible that ISG15 could play a role in the ability of the bronchial epithelium to recover after infection. There have been several recent studies demonstrating both cell-intrinsic and cell-extrinsic mechanisms that are needed to maintain proper airway epithelial integrity. Mice lacking cellular inhibitor of apoptosis 2 (cIAP2) were recently shown to exhibit increased lethality after influenza A virus infection without any observed difference in virus burden or in the immune response to infection (63). Rather, these cIAP2 mice displayed increased necroptosis in the airway epithelium. Innate lymphoid cells have also been reported to protect mice from influenza A virus infection by a manner that is independent of controlling virus replication. These cells secrete amphiregulin, which helps to promote survival by increasing airway epithelial integrity (64). Additional studies will be needed to determine whether ISG15 contributes to these responses.

ISG15 is strongly upregulated after type I interferon stimulation and viral infection, and, in many cases, it protects the host from viral induced morbidity and mortality. Type I interferons have clearly been shown to inhibit virus replication in tissue culture. However, the role of type I interferons during respiratory virus infections *in vivo* is less well understood, and recent findings suggest that the more important role of type I interferons during these infections might be to modulate the immune response to regulate tissue damage and morbidity (53, 55). Similarly, our results suggest that while ISG15 conjugation is capable of antagonizing replication of some viruses, it also plays a role in some aspect of disease tolerance against influenza A virus and Sendai virus infection *in vivo*. Thus, it will be important in the future to more thoroughly evaluate the nonantiviral roles that ISG15 conjugation plays *in vivo* and how these functions might affect disease tolerance and outcome in mice after viral infection.

ACKNOWLEDGMENTS

We thank Xiaohua Jin and Adrianus Boon for helpful discussions and technical assistance.

This study was supported by the NIGMS training grant GM007067 to D.J.M., NIH grant RO1 A1080672 and a Pew Scholar Award to D.J.L., and NIAID AADCRC grant U19-AI070489 to M.J.H. Experimental support was provided by the speed congenic facility of the Rheumatic Disease Core Center (P30 AR048335).

REFERENCES

1. **Biron CA.** 1994. Cytokines in the generation of immune responses to, and resolution of, virus infection. Curr Opin Immunol **6:**530–538. http://dx.doi.org/10.1016/0952-7915(94)90137-6.
2. **Medzhitov R, Schneider DS, Soares MP.** 2012. Disease tolerance as a defense strategy. Science **335:**936–941. http://dx.doi.org/10.1126/science.1214935.
3. **Samuel CE.** 2001. Antiviral actions of interferons. Clin Microbiol Rev **14:**778–809. http://dx.doi.org/10.1128/CMR.14.4.778-809.2001.
4. **Sen GC.** 2001. Viruses and interferons. Annu Rev Microbiol **55:**255–281. http://dx.doi.org/10.1146/annurev.micro.55.1.255.
5. **Stetson DB, Medzhitov R.** 2006. Type I interferons in host defense. Immunity **25:**373–381. http://dx.doi.org/10.1016/j.immuni.2006.08.007.
6. **Schoggins JW, Rice CM.** 2011. Interferon-stimulated genes and their antiviral effector functions. Curr Opin Virol **1:**519–525. http://dx.doi.org/10.1016/j.coviro.2011.10.008.
7. **Goodbourn S, Didcock L, Randall RE.** 2000. Interferons: cell signalling, immune modulation, antiviral response and virus countermeasures. J Gen Virol **81:**2341–2364. http://dx.doi.org/10.1099/vir.0.17157-0.
8. **Korant BD, Blomstrom DC, Jonak GJ, Knight E, Jr.** 1984. Interferon-induced proteins: purification and characterization of a 15,000-dalton protein from human and bovine cells induced by interferon. J Biol Chem **259:**14835–14839.
9. **Der SD, Zhou A, Williams BR, Silverman RH.** 1998. Identification of genes differentially regulated by interferon alpha, beta, or gamma using oligonucleotide arrays. Proc Natl Acad Sci U S A **95:**15623–15628. http://dx.doi.org/10.1073/pnas.95.26.15623.
10. **Knight E, Jr, Fahey D, Cordova B, Hillman M, Kutny R, Reich N, Blomstrom D.** 1988. A 15-kDa interferon-induced protein is derived by COOH-terminal processing of a 17-kDa precursor. J Biol Chem **263:**4520–4522.
11. **Loeb KR, Haas AL.** 1992. The interferon-inducible 15-kDa ubiquitin homolog conjugates to intracellular proteins. J Biol Chem **267:**7806–7813.
12. **Krug RM, Zhao C, Beaudenon S.** 2005. Properties of the ISG15 E1 enzyme UbE1L. Methods Enzymol **398:**32–40. http://dx.doi.org/10.1016/S0076-6879(05)98004-X.
13. **Zhao C, Beaudenon SL, Kelley ML, Waddell MB, Yuan W, Schulman BA, Huibregtse JM, Krug RM.** 2004. The UbcH8 ubiquitin E2 enzyme is also the E2 enzyme for ISG15, an IFN-alpha/beta-induced ubiquitin-like protein. Proc Natl Acad Sci U S A **101:**7578–7582. http://dx.doi.org/10.1073/pnas.0402528101.
14. **Dastur A, Beaudenon S, Kelley M, Krug RM, Huibregtse JM.** 2006. Herc5, an interferon-induced HECT E3 enzyme, is required for conjugation of ISG15 in human cells. J Biol Chem **281:**4334–4338. http://dx.doi.org/10.1074/jbc.M512830200.
15. **Kim KI, Giannakopoulos NV, Virgin HW, Zhang DE.** 2004. Interferon-inducible ubiquitin E2, Ubc8, is a conjugating enzyme for protein ISGylation. Mol Cell Biol **24:**9592–9600. http://dx.doi.org/10.1128/MCB.24.21.9592-9600.2004.
16. **Oudshoorn D, van Boheemen S, Sanchez-Aparicio MT, Rajsbaum R, Garcia-Sastre A, Versteeg GA.** 2012. HERC6 is the main E3 ligase for global ISG15 conjugation in mouse cells. PLoS One **7:**e29870. http://dx.doi.org/10.1371/journal.pone.0029870.
17. **Ketscher L, Basters A, Prinz M, Knobeloch KP.** 2012. mHERC6 is the essential ISG15 E3 ligase in the murine system. Biochem Biophys Res Commun **417:**135–140. http://dx.doi.org/10.1016/j.bbrc.2011.11.071.
18. **Zhao C, Denison C, Huibregtse JM, Gygi S, Krug RM.** 2005. Human ISG15 conjugation targets both IFN-induced and constitutively expressed proteins functioning in diverse cellular pathways. Proc Natl Acad Sci U S A **102:**10200–10205. http://dx.doi.org/10.1073/pnas.0504754102.
19. **Giannakopoulos NV, Luo JK, Papov V, Zou W, Lenschow DJ, Jacobs BS, Borden EC, Li J, Virgin HW, Zhang DE.** 2005. Proteomic identification of proteins conjugated to ISG15 in mouse and human cells. Biochem Biophys Res Commun **336:**496–506. http://dx.doi.org/10.1016/j.bbrc.2005.08.132.
20. **Lenschow DJ, Giannakopoulos NV, Gunn LJ, Johnston C, O'Guin AK, Schmidt RE, Levine B, Virgin HW, IV.** 2005. Identification of interferon-stimulated gene 15 as an antiviral molecule during Sindbis virus infection in vivo. J Virol **79:**13974–13983. http://dx.doi.org/10.1128/JVI.79.22.13974-13983.2005.
21. **Lenschow DJ, Lai C, Frias-Staheli N, Giannakopoulos NV, Lutz A,**

Wolff T, Osiak A, Levine B, Schmidt RE, Garcia-Sastre A, Leib DA, Pekosz A, Knobeloch KP, Horak I, Virgin HWt. 2007. IFN-stimulated gene 15 functions as a critical antiviral molecule against influenza, herpes, and Sindbis viruses. Proc Natl Acad Sci U S A **104:**1371–1376. http://dx.doi.org/10.1073/pnas.0607038104.

22. **Werneke SW, Schilte C, Rohatgi A, Monte KJ, Michault A, Arenzana-Seisdedos F, Vanlandingham DL, Higgs S, Fontanet A, Albert ML, Lenschow DJ.** 2011. ISG15 is critical in the control of Chikungunya virus infection independent of UbE1L mediated conjugation. PLoS Pathog **7:**e1002322. http://dx.doi.org/10.1371/journal.ppat.1002322.
23. **Guerra S, Caceres A, Knobeloch KP, Horak I, Esteban M.** 2008. Vaccinia virus E3 protein prevents the antiviral action of ISG15. PLoS Pathog **4:**e1000096. http://dx.doi.org/10.1371/journal.ppat.1000096.
24. **Lai C, Struckhoff JJ, Schneider J, Martinez-Sobrido L, Wolff T, Garcia-Sastre A, Zhang DE, Lenschow DJ.** 2009. Mice lacking the ISG15 E1 enzyme UbE1L demonstrate increased susceptibility to both mouse-adapted and non-mouse-adapted influenza B virus infection. J Virol **83:**1147–1151. http://dx.doi.org/10.1128/JVI.00105-08.
25. **Hsiang TY, Zhao C, Krug RM.** 2009. Interferon-induced ISG15 conjugation inhibits influenza A virus gene expression and replication in human cells. J Virol **83:**5971–5977. http://dx.doi.org/10.1128/JVI.01667-08.
26. **Zhao C, Hsiang TY, Kuo RL, Krug RM.** 2010. ISG15 conjugation system targets the viral NS1 protein in influenza A virus-infected cells. Proc Natl Acad Sci U S A **107:**2253–2258. http://dx.doi.org/10.1073/pnas.0909144107.
27. **Tang Y, Zhong G, Zhu L, Liu X, Shan Y, Feng H, Bu Z, Chen H, Wang C.** 2010. Herc5 attenuates influenza A virus by catalyzing ISGylation of viral NS1 protein. J Immunol **184:**5777–5790. http://dx.doi.org/10.4049/jimmunol.0903588.
28. **Shi HX, Yang K, Liu X, Liu XY, Wei B, Shan YF, Zhu LH, Wang C.** 2010. Positive regulation of interferon regulatory factor 3 activation by Herc5 via ISG15 modification. Mol Cell Biol **30:**2424–2436. http://dx.doi.org/10.1128/MCB.01466-09.
29. **Durfee LA, Lyon N, Seo K, Huibregtse JM.** 2010. The ISG15 conjugation system broadly targets newly synthesized proteins: implications for the antiviral function of ISG15. Mol Cell **38:**722–732. http://dx.doi.org/10.1016/j.molcel.2010.05.002.
30. **Okumura A, Lu G, Pitha-Rowe I, Pitha PM.** 2006. Innate antiviral response targets HIV-1 release by the induction of ubiquitin-like protein ISG15. Proc Natl Acad Sci U S A **103:**1440–1445. http://dx.doi.org/10.1073/pnas.0510518103.
31. **Woods MW, Kelly JN, Hattlmann CJ, Tong JG, Xu LS, Coleman MD, Quest GR, Smiley JR, Barr SD.** 2011. Human HERC5 restricts an early stage of HIV-1 assembly by a mechanism correlating with the ISGylation of Gag. Retrovirology **8:**95. http://dx.doi.org/10.1186/1742-4690-8-95.
32. **Okumura A, Pitha PM, Harty RN.** 2008. ISG15 inhibits Ebola VP40 VLP budding in an L-domain-dependent manner by blocking Nedd4 ligase activity. Proc Natl Acad Sci U S A **105:**3974–3979. http://dx.doi.org/10.1073/pnas.0710629105.
33. **Malakhova OA, Zhang DE.** 2008. ISG15 inhibits Nedd4 ubiquitin E3 activity and enhances the innate antiviral response. J Biol Chem **283:**8783–8787. http://dx.doi.org/10.1074/jbc.C800030200.
34. **D'Cunha J, Knight E, Jr, Haas AL, Truitt RL, Borden EC.** 1996. Immunoregulatory properties of ISG15, an interferon-induced cytokine. Proc Natl Acad Sci U S A **93:**211–215. http://dx.doi.org/10.1073/pnas.93.1.211.
35. **D'Cunha J, Ramanujam S, Wagner RJ, Witt PL, Knight E, Jr, Borden EC.** 1996. In vitro and in vivo secretion of human ISG15, an IFN-induced immunomodulatory cytokine. J Immunol **157:**4100–4108.
36. **Bogunovic D, Byun M, Durfee LA, Abhyankar A, Sanal O, Mansouri D, Salem S, Radovanovic I, Grant AV, Adimi P, Mansouri N, Okada S, Bryant VL, Kong XF, Kreins A, Velez MM, Boisson B, Khalilzadeh S, Ozcelik U, Darazam IA, Schoggins JW, Rice CM, Al-Muhsen S, Behr M, Vogt G, Puel A, Bustamante J, Gros P, Huibregtse JM, Abel L, Boisson-Dupuis S, Casanova JL.** 2012. Mycobacterial disease and impaired IFN-gamma immunity in humans with inherited ISG15 deficiency. Science **337:**1684–1688. http://dx.doi.org/10.1126/science.1224026.
37. **Kim KI, Yan M, Malakhova O, Luo JK, Shen MF, Zou W, de la Torre JC, Zhang DE.** 2006. Ube1L and protein ISGylation are not essential for alpha/beta interferon signaling. Mol Cell Biol **26:**472–479. http://dx.doi.org/10.1128/MCB.26.2.472-479.2006.
38. **Osiak A, Utermohlen O, Niendorf S, Horak I, Knobeloch KP.** 2005. ISG15, an interferon-stimulated ubiquitin-like protein, is not essential for STAT1 signaling and responses against vesicular stomatitis and lymphocytic choriomeningitis virus. Mol Cell Biol **25:**6338–6345. http://dx.doi.org/10.1128/MCB.25.15.6338-6345.2005.
39. **Neumann G, Watanabe T, Ito H, Watanabe S, Goto H, Gao P, Hughes M, Perez DR, Donis R, Hoffmann E, Hobom G, Kawaoka Y.** 1999. Generation of influenza A viruses entirely from cloned cDNAs. Proc Natl Acad Sci U S A **96:**9345–9350. http://dx.doi.org/10.1073/pnas.96.16.9345.
40. **You Y, Richer EJ, Huang T, Brody SL.** 2002. Growth and differentiation of mouse tracheal epithelial cells: selection of a proliferative population. Am J Physiol Lung Cell Mol Physiol **283:**L1315–L1321.
41. **Damjanovic D, Small CL, Jeyanathan M, McCormick S, Xing Z.** 2012. Immunopathology in influenza virus infection: uncoupling the friend from foe. Clin Immunol **144:**57–69. http://dx.doi.org/10.1016/j.clim.2012.05.005.
42. **La Gruta NL, Kedzierska K, Stambas J, Doherty PC.** 2007. A question of self-preservation: immunopathology in influenza virus infection. Immunol Cell Biol **85:**85–92. http://dx.doi.org/10.1038/sj.icb.7100026.
43. **Tumpey TM, Garcia-Sastre A, Taubenberger JK, Palese P, Swayne DE, Pantin-Jackwood MJ, Schultz-Cherry S, Solorzano A, Van Rooijen N, Katz JM, Basler CF.** 2005. Pathogenicity of influenza viruses with genes from the 1918 pandemic virus: functional roles of alveolar macrophages and neutrophils in limiting virus replication and mortality in mice. J Virol **79:**14933–14944. http://dx.doi.org/10.1128/JVI.79.23.14933-14944.2005.
44. **Perrone LA, Plowden JK, Garcia-Sastre A, Katz JM, Tumpey TM.** 2008. H5N1 and 1918 pandemic influenza virus infection results in early and excessive infiltration of macrophages and neutrophils in the lungs of mice. PLoS Pathog **4:**e1000115. http://dx.doi.org/10.1371/journal.ppat.1000115.
45. **Brandes M, Klauschen F, Kuchen S, Germain RN.** 2013. A systems analysis identifies a feedforward inflammatory circuit leading to lethal influenza infection. Cell **154:**197–212. http://dx.doi.org/10.1016/j.cell.2013.06.013.
46. **Kobasa D, Takada A, Shinya K, Hatta M, Halfmann P, Theriault S, Suzuki H, Nishimura H, Mitamura K, Sugaya N, Usui T, Murata T, Maeda Y, Watanabe S, Suresh M, Suzuki T, Suzuki Y, Feldmann H, Kawaoka Y.** 2004. Enhanced virulence of influenza A viruses with the haemagglutinin of the 1918 pandemic virus. Nature **431:**703–707. http://dx.doi.org/10.1038/nature02951.
47. **Garcia-Sastre A, Durbin RK, Zheng H, Palese P, Gertner R, Levy DE, Durbin JE.** 1998. The role of interferon in influenza virus tissue tropism. J Virol **72:**8550–8558.
48. **Look DC, Walter MJ, Williamson MR, Pang L, You Y, Sreshta JN, Johnson JE, Zander DS, Brody SL.** 2001. Effects of paramyxoviral infection on airway epithelial cell Foxj1 expression, ciliogenesis, and mucociliary function. Am J Pathol **159:**2055–2069. http://dx.doi.org/10.1016/S0002-9440(10)63057-X.
49. **Buchweitz JP, Harkema JR, Kaminski NE.** 2007. Time-dependent airway epithelial and inflammatory cell responses induced by influenza virus A/PR/8/34 in C57BL/6 mice. Toxicol Pathol **35:**424–435. http://dx.doi.org/10.1080/01926230701302558.
50. **Ibricevic A, Pekosz A, Walter MJ, Newby C, Battaile JT, Brown EG, Holtzman MJ, Brody SL.** 2006. Influenza virus receptor specificity and cell tropism in mouse and human airway epithelial cells. J Virol **80:**7469–7480. http://dx.doi.org/10.1128/JVI.02677-05.
51. **Yuan W, Krug RM.** 2001. Influenza B virus NS1 protein inhibits conjugation of the interferon (IFN)-induced ubiquitin-like ISG15 protein. EMBO J **20:**362–371. http://dx.doi.org/10.1093/emboj/20.3.362.
52. **Sridharan H, Zhao C, Krug RM.** 2010. Species specificity of the NS1 protein of influenza B virus: NS1 binds only human and non-human primate ubiquitin-like ISG15 proteins. J Biol Chem **285:**7852–7856. http://dx.doi.org/10.1074/jbc.C109.095703.
53. **Davidson S, Crotta S, McCabe TM, Wack A.** 2014. Pathogenic potential of interferon αβ in acute influenza infection. Nat Commun **5:**3864. http://dx.doi.org/10.1038/ncomms4864.
54. **Lopez CB, Yount JS, Hermesh T, Moran TM.** 2006. Sendai virus infection induces efficient adaptive immunity independently of type I interferons. J Virol **80:**4538–4545. http://dx.doi.org/10.1128/JVI.80.9.4538-4545.2006.
55. **Seo SU, Kwon HJ, Ko HJ, Byun YH, Seong BL, Uematsu S, Akira S, Kweon MN.** 2011. Type I interferon signaling regulates Ly6C(hi) monocytes and neutrophils during acute viral pneumonia in mice. PLoS Pathog **7:**e1001304. http://dx.doi.org/10.1371/journal.ppat.1001304.
56. **Shahangian A, Chow EK, Tian X, Kang JR, Ghaffari A, Liu SY, Belperio JA, Cheng G, Deng JC.** 2009. Type I IFNs mediate development of

postinfluenza bacterial pneumonia in mice. J Clin Invest **119:**1910–1920. http://dx.doi.org/10.1172/JCI35412.

57. **Robinson TW, Cureton RJ, Heath RB.** 1968. The pathogenesis of Sendai virus infection in the mouse lung. J Med Microbiol **1:**89–95. http://dx.doi.org/10.1099/00222615-1-1-89.
58. **Parker JC, Whiteman MD, Richter CB.** 1978. Susceptibility of inbred and outbred mouse strains to Sendai virus and prevalence of infection in laboratory rodents. Infect Immun **19:**123–130.
59. **Jeon YJ, Choi JS, Lee JY, Yu KR, Kim SM, Ka SH, Oh KH, Kim KI, Zhang DE, Bang OS, Chung CH.** 2009. ISG15 modification of filamin B negatively regulates the type I interferon-induced JNK signalling pathway. EMBO Rep **10:**374–380. http://dx.doi.org/10.1038/embor.2009.23.
60. **Yanguez E, Garcia-Culebras A, Frau A, Llompart C, Knobeloch KP, Gutierrez-Erlandsson S, Garcia-Sastre A, Esteban M, Nieto A, Guerra S.** 2013. ISG15 regulates peritoneal macrophages functionality against viral infection. PLoS Pathog **9:**e1003632. http://dx.doi.org/10.1371/journal.ppat.1003632.
61. **Roulston A, Marcellus RC, Branton PE.** 1999. Viruses and apoptosis. Annu Rev Microbiol **53:**577–628. http://dx.doi.org/10.1146/annurev.micro.53.1.577.
62. **Desai SD, Reed RE, Burks J, Wood LM, Pullikuth AK, Haas AL, Liu LF, Breslin JW, Meiners S, Sankar S.** 2012. ISG15 disrupts cytoskeletal architecture and promotes motility in human breast cancer cells. Exp Biol Med **237:**38–49. http://dx.doi.org/10.1258/ebm.2011.011236.
63. **Rodrigue-Gervais IG, Labbe K, Dagenais M, Dupaul-Chicoine J, Champagne C, Morizot A, Skeldon A, Brincks EL, Vidal SM, Griffith TS, Saleh M.** 2014. Cellular inhibitor of apoptosis protein cIAP2 protects against pulmonary tissue necrosis during influenza virus infection to promote host survival. Cell Host Microbe **15:**23–35. http://dx.doi.org/10.1016/j.chom.2013.12.003.
64. **Monticelli LA, Sonnenberg GF, Abt MC, Alenghat T, Ziegler CG, Doering TA, Angelosanto JM, Laidlaw BJ, Yang CY, Sathaliyawala T, Kubota M, Turner D, Diamond JM, Goldrath AW, Farber DL, Collman RG, Wherry EJ, Artis D.** 2011. Innate lymphoid cells promote lung-tissue homeostasis after infection with influenza virus. Nat Immunol **12:**1045–1054. http://dx.doi.org/10.1038/ni.2131.